

COMPUTATION OF THREE-DIMENSIONAL TRANSONIC FLOWS USING TWO STREAM FUNCTIONS

A. SHERIF

Cairo University, Cairo, Egypt

AND

M. HAFEZ

University of California, Davis, CA, 95616, U.S.A.

SUMMARY

A computational method for three-dimensional flows is presented in terms of two stream functions, which may be considered as two components of a generalized vector potential. An iterative scheme is developed such that only a sequence of two-dimensional-like problems, for each function, is solved. The convergence of the iterative scheme is studied based on von Neumann linear analysis. For transonic flow calculation, numerical methods used for potential flows are readily applied, namely artificial density and Zebra relaxation. Results of transonic flow calculations around a wing are presented.

KEY WORDS Three-dimensional transonic flows Vector potential

INTRODUCTION

In general, three-dimensional calculations are expensive and, for some configurations, approximate models are useful for engineering purposes. For example, Wu¹ suggested solving three-dimensional turbomachinery problems using two stream functions defined on blade-to-blade and hub-to-shroud surfaces. Due to the approximations in his analysis, only quasi-three-dimensional effects are accounted for. Another classical example of approximate models is the use of asymptotic wing theories.² For high-aspect-ratio wings, the lifting-line concept to Prandtl is a practical tool. In these cases, only two-dimensional calculations are needed and the three-dimensional effect is produced through the induced angle of attack. For low-aspect-ratio wings, in the transonic regime, the area rule of Oswatitsch offers a great simplification. Far from the wing, the flow field is similar to that around a body of revolution with the same cross-sectional area distribution; hence only an axisymmetric flow calculation is needed.

Because of the rapid progress in computer technology, full three-dimensional calculations are feasible, and accurate prediction of flow fields is obtained without such approximations. The above models, however, could be useful in constructing efficient iterative algorithms to solve more general cases.³ Such algorithms should also be capable of treating the full three-dimensional problem in its complete form.

In this paper, a method is presented for calculating three-dimensional transonic flows through a sequence of two-dimensional-like problems. Results are presented only for irrotational flows.

Possible extensions to treat rotational effects are discussed. For convenience, linearized boundary conditions are used, but this is not, of course, a restriction to the present method.

FORMULATION OF THE PROBLEM

In Reference 4, the stream function equation for transonic two-dimensional flows is solved and a technique is presented to overcome the main difficulty of such a formulation; namely, that the density is not uniquely determined in terms of the flux, since there are two solutions—the subsonic and the supersonic branches, with a square root singularity at the sonic point. Differential, integral and variational formulations of rotational flows are presented. Numerical results based on the artificial density method⁵ and a Zebra relaxation^{6,7} procedure are compared with Euler and potential solutions. In general, stream function calculations are almost as fast as the potential (the convergence rate is faster, but the computational rate is slightly lower due to the density complications). On the other hand, existing Euler calculations, explicit and implicit, are much slower (and the computational rate is at least twice as slow). Extension to three-dimensional flows in terms of two stream functions is also briefly discussed in Reference 4. In this paper, a different approach is used, which offers some simplifications. In the following, a comparison between the two approaches is given.

THE FIRST APPROACH

The flux vector $\rho\mathbf{q}$ can be presented in terms of two stream functions ψ and θ as⁴

$$\rho\mathbf{q} = \nabla\psi \times \nabla\theta. \quad (1)$$

Thus the continuity equation is automatically satisfied, since

$$\nabla \cdot (\rho\mathbf{q}) = \nabla \cdot (\nabla\psi \times \nabla\theta) = 0. \quad (2)$$

In terms of Cartesian co-ordinates, the velocity components u, v and w are defined by

$$u = (\psi_y\theta_z - \theta_y\psi_z)/\rho, \quad v = (-\psi_x\theta_x + \theta_x\psi_z)/\rho, \quad w = (\psi_x\theta_y - \theta_x\psi_y)/\rho, \quad (3)$$

and the governing differential equations are

$$w_y - v_z = \omega_1, \quad u_x - w_x = \omega_2, \quad v_x - u_y = \omega_3 \quad (4)$$

or

$$\begin{aligned} \left(\frac{\theta_{y\alpha}}{\rho}\right)_y + \left(\frac{\theta_{z\alpha}}{\rho}\right)_z &= \left(\frac{\psi_{y\bar{\alpha}}}{\rho}\right)_y + \left(\frac{\psi_{z\bar{\alpha}}}{\rho}\right)_z + \omega_1, \\ \left(\frac{\theta_{z\beta}}{\rho}\right)_z + \left(\frac{\theta_{x\beta}}{\rho}\right)_x &= \left(\frac{\psi_{x\bar{\beta}}}{\rho}\right)_z + \left(\frac{\psi_{x\bar{\beta}}}{\rho}\right)_x + \omega_2, \\ \left(\frac{\theta_{x\gamma}}{\rho}\right)_x + \left(\frac{\theta_{y\gamma}}{\rho}\right)_y &= \left(\frac{\psi_{y\bar{\gamma}}}{\rho}\right)_x + \left(\frac{\psi_{y\bar{\gamma}}}{\rho}\right)_y + \omega_3, \end{aligned} \quad (5)$$

where

$$\alpha = \psi_x, \quad \bar{\alpha} = \theta_x, \quad \beta = \psi_y, \quad \bar{\beta} = \theta_y, \quad \gamma = \psi_z, \quad \bar{\gamma} = \theta_z.$$

$\boldsymbol{\omega} = \nabla \times \mathbf{q}$ and hence $\nabla \cdot \boldsymbol{\omega} = 0$ or

$$\omega_{1x} + \omega_{2y} + \omega_{3z} = 0. \quad (6)$$

Any two equations of (5) can be solved for ψ and θ . The above system reduces to the usual two-

dimensional case when, for example, $\theta = z$ and $\psi = \psi(x, y)$.

If the equation of the body is

$$B(x, y, z) = 0, \quad (7)$$

the boundary condition is

$$\nabla\psi \times \nabla\theta \cdot \nabla B = 0; \quad (8)$$

i.e., the body is a stream surface.

Some choices of iterative algorithms are obvious from the way the equations are written. Comparing with the potential formulation, for example, the computational rate will be definitely unfavourable due to the number of terms involved.

THE SECOND APPROACH

Another approach is based on the vector potential, where, according to the Helmholtz theorem, any vector can be represented as the gradient of a scalar plus the curl of another vector which is divergence-free. In other words, a vector field is completely determined if all its sources and all its vortices are given.⁸ For incompressible flows,

$$\nabla \cdot \mathbf{q} = S \quad (9)$$

and

$$\nabla \times \mathbf{q} = \boldsymbol{\omega}. \quad (10)$$

If

$$\mathbf{q} = -\nabla\phi + \nabla \times \boldsymbol{\psi}, \quad (11)$$

where ϕ is a scalar and $\boldsymbol{\psi}$ is a vector, such that $\nabla \cdot \boldsymbol{\psi} = 0$, equations (9) and (10) reduce to

$$-\nabla^2 \phi = S, \quad (9')$$

$$-\nabla^2 \boldsymbol{\psi} = \boldsymbol{\omega}, \quad (10')$$

since $\nabla \times (\nabla \times \boldsymbol{\psi}) = \nabla(\nabla \cdot \boldsymbol{\psi}) - \nabla^2 \boldsymbol{\psi}$. For a flow around a closed body, where there are no sources in the field ($S = 0$), ϕ can vanish everywhere.

Similarly, for compressible flows,

$$\nabla \cdot \rho \mathbf{q} = S \quad (12)$$

and

$$\nabla \times \mathbf{q} = \boldsymbol{\omega}. \quad (13)$$

Let

$$\rho \mathbf{q} = -\rho \nabla\phi + \nabla \times \boldsymbol{\psi}, \quad (14')$$

where ϕ is scalar and $\boldsymbol{\psi}$ is a vector. Equations (12) and (13) reduce to

$$-\nabla \cdot \rho \nabla\phi = S, \quad (12')$$

$$\nabla \times (\nabla \times \boldsymbol{\psi})/\rho = \boldsymbol{\omega}. \quad (13')$$

Again, ϕ can vanish identically if $S = 0$.

In terms of Cartesian co-ordinates (the corresponding equation in generalized co-ordinates is given in the Appendix), the velocity components u , v and w are defined by

$$u = (\psi_{3y} - \psi_{2z})/\rho, \quad v = (-\psi_{3x} + \psi_{1z})/\rho, \quad w = (\psi_{2x} - \psi_{1y})/\rho \quad (15)$$

and the governing differential equations become

$$\begin{aligned}(\psi_{1y}/\rho)_y + (\psi_{1z}/\rho)_z &= (\psi_{2x}/\rho)_y + (\psi_{3x}/\rho)_z - \omega_1, \\(\psi_{2x}/\rho)_x + (\psi_{2z}/\rho)_z &= (\psi_{1y}/\rho)_x + (\psi_{3y}/\rho)_z - \omega_2, \\(\psi_{3x}/\rho)_x + (\psi_{3y}/\rho)_y + (\psi_{1z}/\rho)_x + (\psi_{2z}/\rho)_y &= \omega_3.\end{aligned}\tag{16}$$

For the two-dimensional case, ψ_1, ψ_2, ω_1 and ω_2 vanish identically. The boundary condition is

$$(\nabla \times \boldsymbol{\psi}) \cdot \nabla B = 0\tag{17}$$

or

$$(\psi_{3y} - \psi_{2z})B_x + (-\psi_{3x} + \psi_{1z})B_y + (\psi_{2x} - \psi_{1y})B_z = 0.\tag{17'}$$

FURTHER SIMPLIFICATIONS

Although it is preferable to have symmetry in equations (16), in particular when there is a strong coupling between the different components of the vorticity, it is not necessary, for steady state calculations, to keep the three functions ψ_1, ψ_2 and ψ_3 . One of the components of the vector potential $\boldsymbol{\psi}$ can be set equal to zero everywhere. For example, if ψ_1 is chosen to be zero, the velocity is defined by

$$\boldsymbol{u} = (\tilde{\psi}_{3y} - \psi_{2z})/\rho, \quad \boldsymbol{v} = -\tilde{\psi}_{3x}/\rho, \quad \boldsymbol{w} = \tilde{\psi}_{2x}/\rho\tag{15'}$$

and the governing equations are

$$\begin{aligned}(\tilde{\psi}_{2x}/\rho)_x + (\tilde{\psi}_{2z}/\rho)_z &= (\tilde{\psi}_{3y}/\rho)_z - \omega_2, \\(\tilde{\psi}_{3x}/\rho)_x + (\tilde{\psi}_{3y}/\rho)_y &= (\tilde{\psi}_{2z}/\rho)_y - \omega_3,\end{aligned}\tag{16'}$$

where the equation for ω_1 is now in terms of $\tilde{\psi}_2$ and $\tilde{\psi}_3$ only and the boundary condition is

$$(\tilde{\psi}_{3y} - \tilde{\psi}_{2z})B_x + (-\tilde{\psi}_{3x})B_y + (\tilde{\psi}_{2x})B_z = 0.\tag{17''}$$

Obviously, the simplified system (ψ_2, ψ_3) is a special case; the relation to the more general formulation (ψ_1, ψ_2, ψ_3) is

$$\tilde{\psi}_3 = \psi_3 - \int \psi_{1z} dx, \quad \tilde{\psi}_2 = \psi_2 - \int \psi_{1y} dx,\tag{18}$$

provided

$$\left(\int \psi_{1z} dx \right)_y = \left(\int \psi_{1y} dx \right)_z.\tag{19}$$

Condition (19) is satisfied by most practical flows.⁹

Notice that, unlike the functions ψ and θ which appear in (3), (5) and (8), $\psi_2 = \text{constant}$ and $\psi_3 = \text{constant}$ are no longer physical stream surfaces. The terms $(\tilde{\psi}_{3y}/\rho)_z$ and $(\tilde{\psi}_{2z}/\rho)_y$ represent the cross-flow effects and are responsible for the three-dimensional coupling.

LEAST-SQUARES AND VARIATIONAL PRINCIPLE FOR ROTATIONAL FLOWS

It is noticed in Reference 10 that the vector potential formulations can be obtained in an alternative way without using explicitly the Helmholtz theorem. In Cartesian co-ordinates, equations (12) and (13) become

$$\begin{aligned}(\rho u)_x + (\rho v)_y + (\rho w)_z &= S, \\v_x - u_y &= \omega_3, \quad -w_x + u_z = \omega_2, \quad w_y - v_z = \omega\end{aligned}$$

or, in matrix-vector notation,

$$\begin{pmatrix} \partial_x \rho & \partial_y \rho & \partial_z \rho \\ -\partial_y & \partial_x & 0 \\ \partial_z & 0 & -\partial_x \\ 0 & -\partial_z & \partial_y \end{pmatrix} \begin{pmatrix} u \\ v \\ w \end{pmatrix} = \begin{pmatrix} S \\ \omega_3 \\ \omega_2 \\ \omega_1 \end{pmatrix}. \quad (20)$$

The previous system is overdetermined (four equations and three unknowns). If least squares are used, derivatives of u , v , w and ω require special treatment if they are not continuous; thus the following functions are introduced through the adjoint operator as

$$\begin{pmatrix} -\rho \partial_x & \partial_y & -\partial_z & 0 \\ -\rho \partial_y & -\partial_x & 0 & +\partial_z \\ -\rho \partial_z & 0 & +\partial_x & -\partial_y \end{pmatrix} \begin{pmatrix} \phi \\ \psi_3 \\ \psi_2 \\ \psi_1 \end{pmatrix} = \begin{pmatrix} \rho u \\ \rho v \\ \rho w \end{pmatrix} \quad (21)$$

or

$$-\rho \phi_x + \psi_{3y} - \psi_{2z} = \rho u, \quad -\rho \phi_y - \psi_{3x} + \psi_{1z} = \rho v, \quad -\rho \phi_z + \psi_{2x} - \psi_{1y} = \rho w. \quad (21')$$

If ϕ is chosen zero (when $S = 0$), equations (21') becomes the same as equations (15). Similarly, if ψ_1 is chosen to be zero, the simplified equations (15') are obtained.

It should be mentioned that there is a variational principle (at least for subsonic flows). As discussed in Reference 4, the functional $I = \int_V p + \rho q^2 dV$ is stationary and, through minimization, the governing differential equations and the associated natural boundary conditions are obtained.

GLOBAL ITERATIVE PROCESS FOR THE COUPLED STREAM FUNCTION EQUATIONS

Since the coupled system of equations for the stream functions can be derived from a least-squares procedure, standard iterative techniques (Jacobi, Gauss-Seidel and successive over-relaxation) should converge. A von Neumann analysis for incompressible flows confirms this conclusion.

Consider the splitting

$$\begin{aligned} (\psi_{2x}/\rho)_x^{n+1} + (\psi_{2z}/\rho)_z^{n+1} &= (\psi_{3y}/\rho)_y^n - \omega_2, \\ (\psi_{3x}/\rho)_x^{n+1} (\psi_{3y}/\rho)_y^{n+1} &= (\psi_{2z}/\rho)_z^n - \omega_3. \end{aligned}$$

Let

$$\delta\psi_2 = g_2^n e^{i(\xi x + \eta y + \zeta z)}, \quad (22)$$

$$\delta\psi_3 = g_3^n e^{i(\xi x + \eta y + \zeta z)}, \quad (23)$$

where $\delta\psi_2$ and $\delta\psi_3$ are the differences between the n -iterates and the exact solution. Substituting (23) in (22) yields ($\rho = 1$)

$$\begin{pmatrix} -(\xi^2 + \eta^2) & 0 \\ 0 & -(\xi^2 + \eta^2) \end{pmatrix} \begin{pmatrix} g_2^{n+1} \\ g_3^{n+1} \end{pmatrix} = \begin{pmatrix} 0 & -\eta\zeta \\ -\eta\zeta & 0 \end{pmatrix} \begin{pmatrix} g_2^n \\ g_3^n \end{pmatrix}$$

or

$$g_2^{n+1} = \lambda^2 g_2^{n-1}, \quad g_3^{n+1} = \lambda^2 g_3^{n-1}, \quad (24)$$

where

$$\lambda^2 = \frac{\eta^2 \zeta^2}{(\xi^2 + \zeta^2)(\xi^2 + \eta^2)} \leq 1.$$

A faster convergence is expected if the most recent value of ψ_2 is used in the right-hand side of the

ψ_3 equation. Indeed, a Gauss–Seidel iteration is twice as fast and over-relaxation will further improve the convergence.

In the actual calculations, inner and outer iterations are used to solve for ψ_2^{n+1} and ψ_3^{n+1} . Because of non-linearity, only a few inner iterations for each outer iteration are used. It should be mentioned that a two-dimensional splitting for a 3D potential equation is not recommended, since the iteration based on equation (25),

$$\phi_{xx}^{n+1} + \phi_{yy}^{n+1} = -\phi_{zz}^n, \quad (25)$$

may not converge for general three-dimensional problems.

COMPUTATIONAL ALGORITHMS

The equations in conservation form are discretized using finite differences. For transonic flows, an artificial viscosity is added through modifying the density⁴:

$$\tilde{\rho} = \rho - \mu \rho_s \Delta s, \quad (26)$$

where

$$\rho_s \Delta s = \frac{u}{q} \rho_x \Delta x + \frac{v}{q} \rho_y \Delta y.$$

The switching factor μ is expressed in terms of ρ to avoid repeated calculations of the Mach numbers; i.e.,

$$\mu = \varepsilon \max [0, 1 - (\rho/\rho_c)^n], \quad (27)$$

where ρ_c is the critical value of the density or a cut-off value close to the sonic condition. The exponent n is chosen to be 1. The factor ε controls the amount of viscosity.

Following Reference 4, the algorithm described in Figure 1 is used. In these calculations, it is

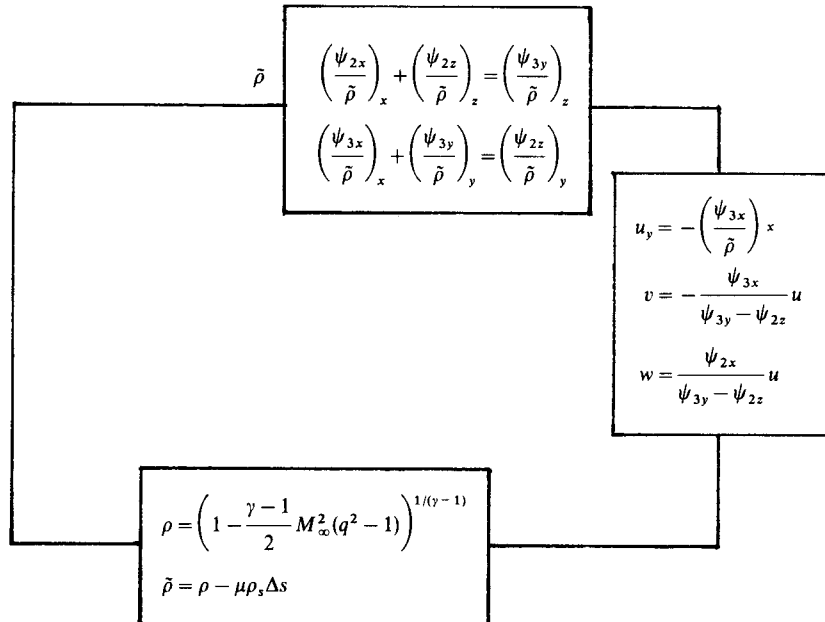


Figure 1. Iterative algorithm for mixed flows

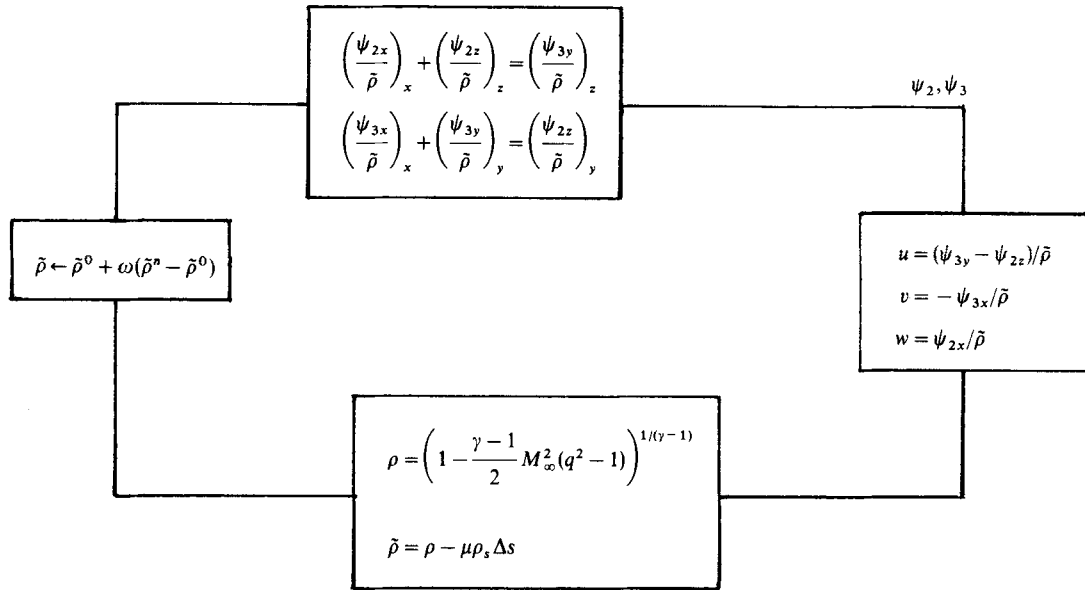


Figure 2. A simple iterative algorithm

assumed that the three-dimensional effects are a perturbation (not necessarily small) on the two-dimensional flow component in the xy plane.

A simpler procedure is described in Figure 2. In general, such an algorithm is used only for subsonic flows. If ρ is under-relaxed and more artificial viscosity is added, the simple algorithm converges even for difficult transonic cases.

TRANSONIC FLOWS AROUND AEROFOILS AND WINGS

Consider first an irrotational two-dimensional flow around a wing section. The far-field boundary condition is given in terms of the circulation Γ ($\rho_\infty = q_\infty = 1$):

$$\psi = y \cos \alpha - x \sin \alpha + \frac{\beta \Gamma}{4\pi} \ln(x^2 + \beta^2 y^2), \quad (28)$$

where $\beta^2 = 1 - M_\infty^2$ and α is the angle of attack. Γ is calculated by integrating the velocity along the aerofoil:

$$\Gamma = \oint q \, dS. \quad (29)$$

The other boundary condition is that the aerofoil is a streamline, $\psi = C$; C is not known *a priori*.

Together with the Kutta condition, the formulation is complete. In Reference 11, exact boundary conditions and body-fitted co-ordinates are used. In the present work only linearized boundary conditions along a slit are considered. The unknown constant C is calculated to guarantee that ψ_y is the same on the top and the bottom of the aerofoil at the trailing edge; so, as a first order approximation,

$$C = [\psi(x_{TE}, +h) + \psi(x_{TE}, -h)]/2, \quad (30)$$

where h is the grid size.

South¹² suggested that, if the outer boundary is chosen such that $x^2 + \beta^2 y^2$ is approximately constant, the contribution of the vortex is just a constant which can be subtracted everywhere. Thus the outer boundary condition does not vary with iteration, leading to reliable convergence.

For a three-dimensional flow around a wing, the linearized condition is (where x is in the flow direction and z along the spanwise direction)

$$f_x = -\psi_{3x} \tag{31}$$

or

$$f = -\psi_3 + C(z). \tag{31'}$$

Transferring these conditions to the plane $y = 0$ yields, on the upper and lower sides respectively,

$$\psi_{3u} = C(z) - f_u(x, y), \quad \psi_{3l} = C(z) + f_l(x, z).$$

The Kutta condition is used in the same way as in the two-dimensional case, where at each spanwise location the small disturbance condition is simply

$$u_u = u_l \tag{32}$$

or

$$(\psi_{3y} - \psi_{2z})_u = (\psi_{3y} - \psi_{2z})_l. \tag{32'}$$

In the far field, the flow is uniform and ψ_2 vanishes there. In the plane $y = 0$ on the wing surface and the vortex sheet, ψ_2 is calculated by averaging the corresponding values above and below this particular plane.

Numerical results for two-dimensional subsonic and transonic lifting and non-lifting flows are plotted in Figure 3. Comparisons with other results, potential and stream function solutions, are included.

In Figures 4 and 5, three-dimensional results are compared with those of Reference 13.

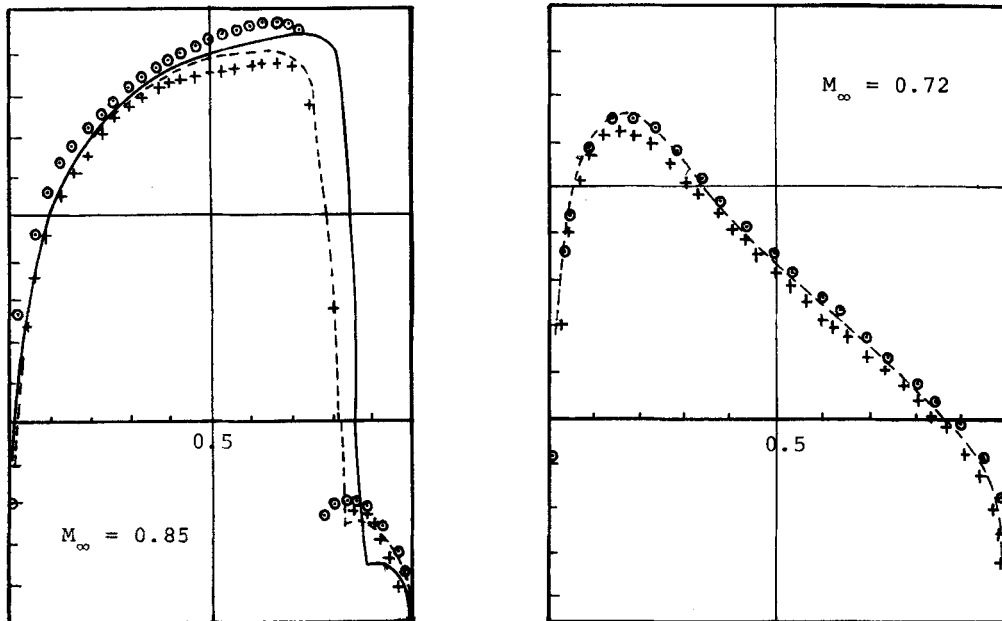


Figure 3(a). Section pressure distribution for an infinite wing compared with other two-dimensional solutions¹⁶ for NACA0012:—Jameson;----Holst; 2-D stream function + exact B.C.; ○ present

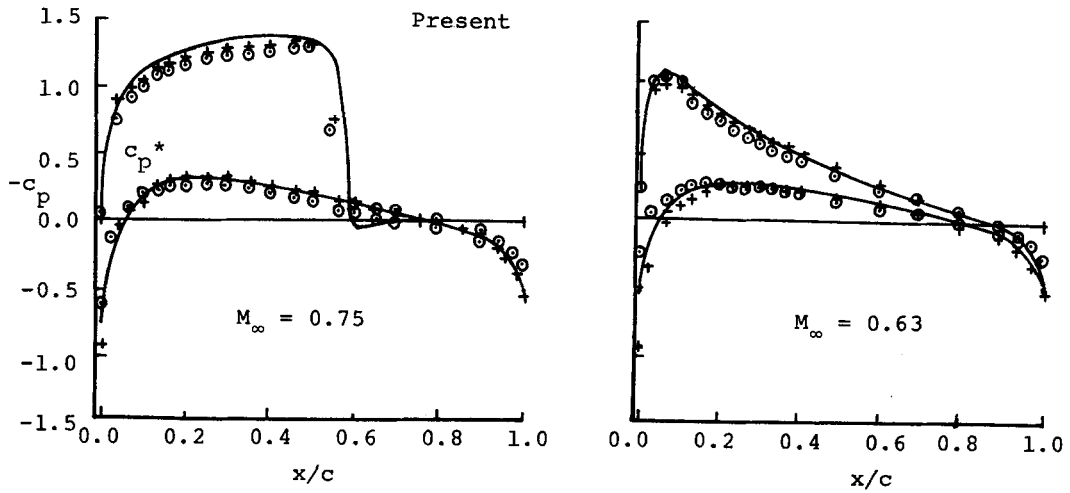


Figure 3(b). Section pressure coefficient for lifting an infinite wing compared to two-dimensional solutions ($\alpha = 2^\circ$):
 ——— Bridgeman and Steger; + 2-D stream function + exact B.C.; \odot present

Convergence histories for the two stream functions are given in Figure 6.

CONCLUSIONS

Three-dimensional irrotational transonic flow around a wing is calculated in terms of two stream functions. Extension to rotational flows requires shock detection to evaluate the entropy function and hence the generated vorticity. Also, vorticity generated due to the variation of the total enthalpy can be treated; e.g., wings in non-uniform flows. In Reference 14, three-dimensional viscous flows are simulated using two stream functions, but only incompressible flows are considered. Work is in progress to combine the present transonic capability with the viscous flow calculations.

APPENDIX. STREAM FUNCTION EQUATIONS IN GENERALIZED CO-ORDINATES

Let x^i be a system of Cartesian co-ordinates, y^i be a system of curvilinear co-ordinates and \mathbf{e}_j be the natural tangent vectors to the co-ordinate curves y^i .

In three dimensions, the curl of a vector field $\boldsymbol{\psi} = (\psi_1, \psi_2, \psi_3)$ is given by (see Reference 15)

$$\text{curl } \boldsymbol{\psi} = \frac{\varepsilon^{ijk}}{g} \frac{\partial \psi_j}{\partial y^i} \mathbf{e}_k, \quad (33)$$

where Einstein summation conventions have been employed and ε^{ijk} is defined by

$$\mathbf{e}_i \times \mathbf{e}_j = \frac{\varepsilon^{ijk}}{g} \mathbf{e}_k$$

and $\varepsilon_{ijk} = g\varepsilon^{ijk}$, with

$$g_{ij} = \mathbf{e}_i \cdot \mathbf{e}_j = \frac{\partial x^k}{\partial y^i} \cdot \frac{\partial x^k}{\partial y^j}, \quad g - J^2 = [\det(\partial x^i / \partial y^i)]^2.$$

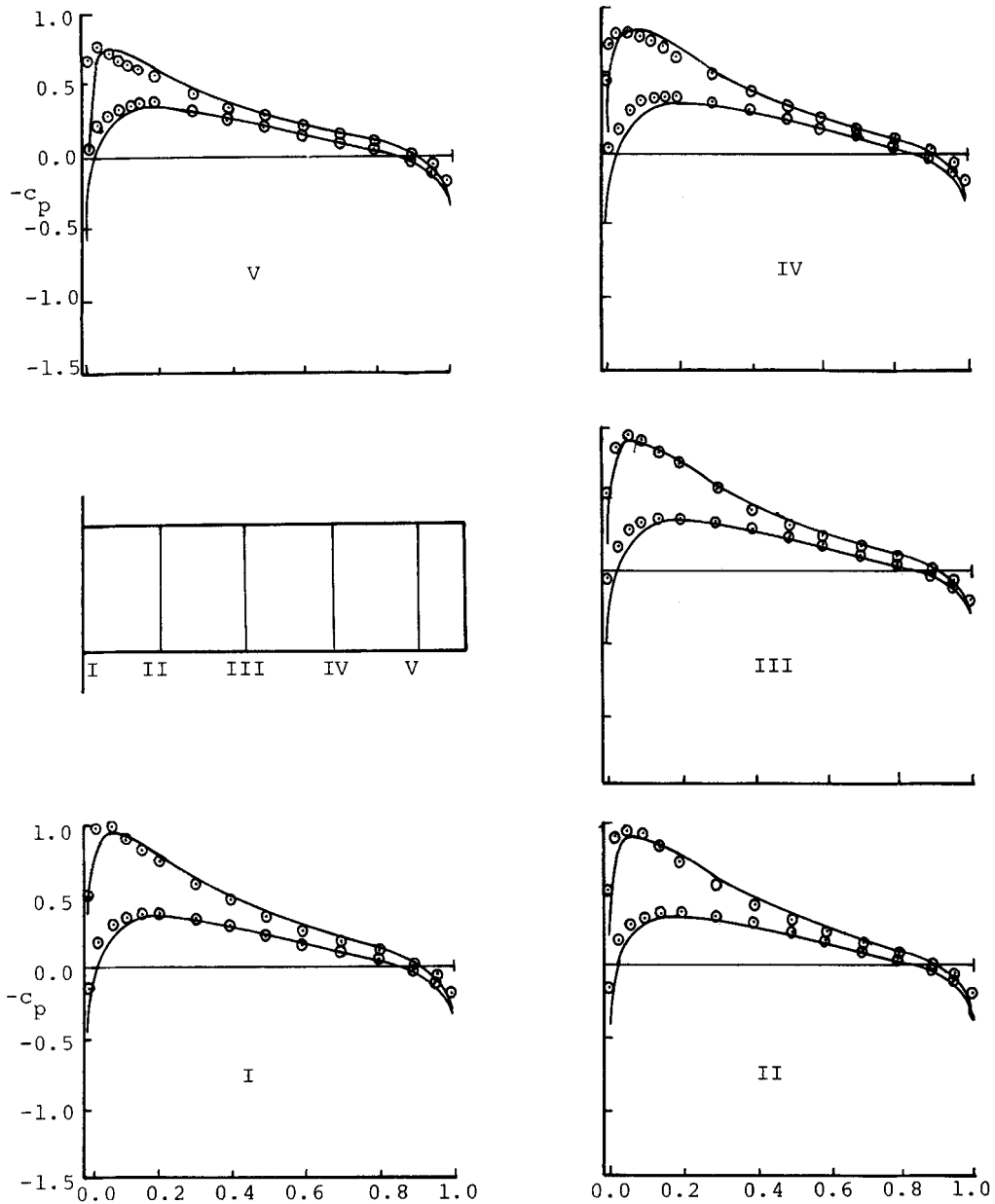


Figure 4. Comparison of the distributions of section pressure coefficient for a NACA 0012 lifting rectangular wing: $AR = 6, M_\infty = 0.63, \alpha = 2^\circ$

The flux vector $\rho \mathbf{q}$ is defined as

$$\rho \mathbf{q} = \text{curl } \psi,$$

giving

$$\mathbf{q} = (q^1, q^2, q^3) = \frac{1}{\rho \sqrt{g}} \left(\frac{\partial \psi_3}{\partial y^2} - \frac{\partial \psi_2}{\partial y^3}, \frac{\partial \psi_1}{\partial y^3} - \frac{\partial \psi_3}{\partial y^1}, \frac{\partial \psi_2}{\partial y^3} - \frac{\partial \psi_1}{\partial y^2} \right). \quad (34)$$

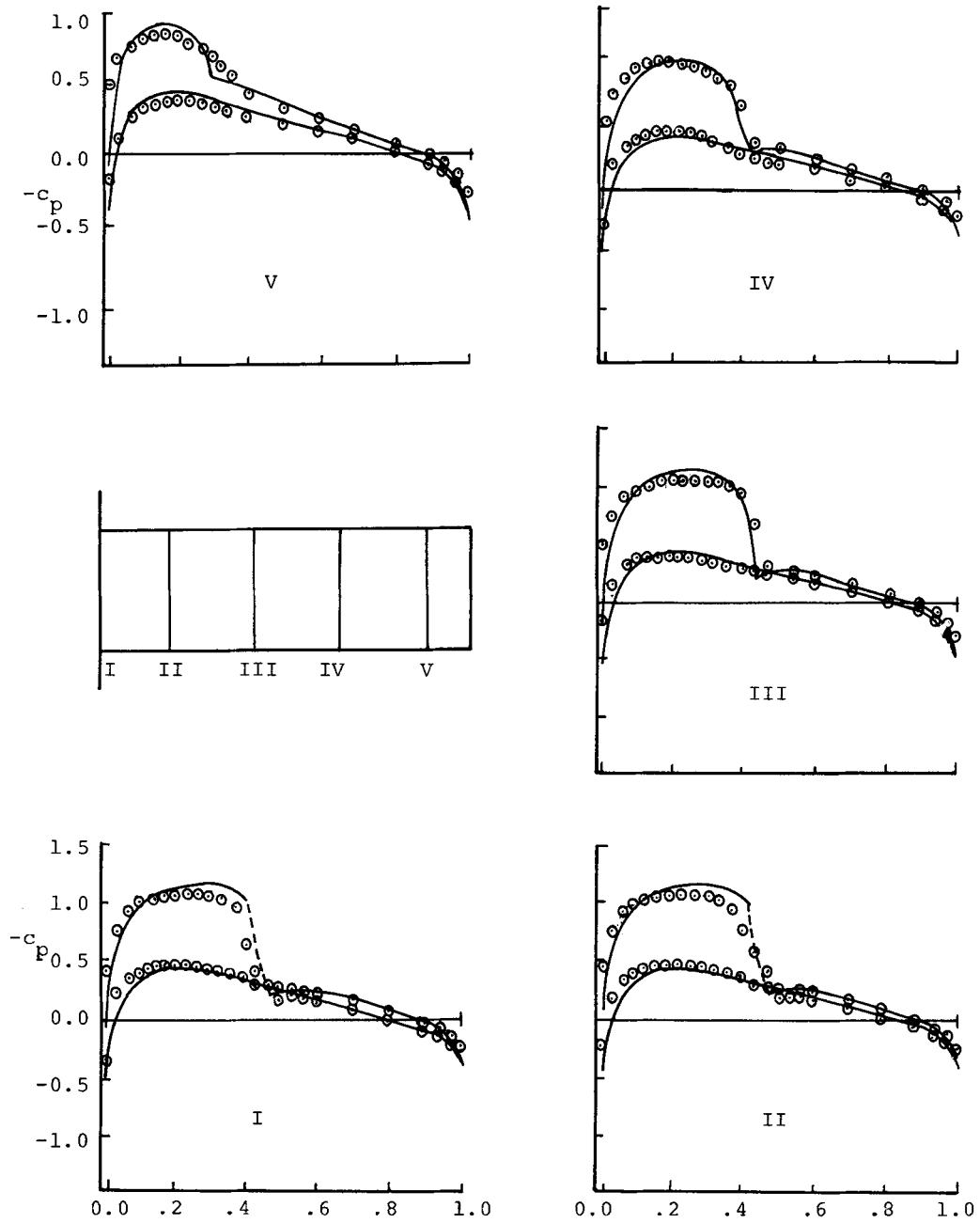


Figure 5. Comparison of the distributions of section pressure coefficient for a NACA 0012 lifting rectangular wing; $AR = 6, M_\infty = 0.75, \alpha = 2^\circ$, grid (81, 51, 12)

The covariant velocity components are obtained from (34) through

$$q_i = g_{ij}q^j \tag{35}$$

or, in expanded form,

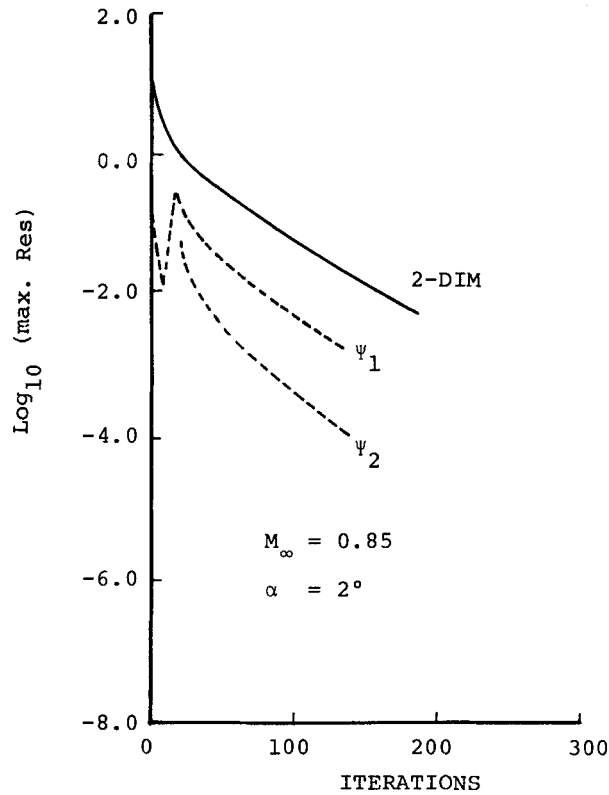


Figure 6. Convergence histories for the residuals of ψ_1 and ψ_2 compared with a two-dimensional calculation

$$\begin{pmatrix} q_1 \\ q_2 \\ q_3 \end{pmatrix} = \begin{pmatrix} g_{11} & g_{12} & g_{13} \\ g_{21} & g_{22} & g_{23} \\ g_{31} & g_{32} & g_{33} \end{pmatrix} \begin{pmatrix} q_1 \\ q_2 \\ q_3 \end{pmatrix}. \quad (36)$$

The vorticity is then defined as

$$\omega = \text{curl } \mathbf{q} = \frac{1}{g} \left(\frac{\partial q_3}{\partial y^2} - \frac{\partial q_2}{\partial y^3}, \frac{\partial q_1}{\partial y^3} - \frac{\partial q_3}{\partial y^1}, \frac{\partial q_2}{\partial y^1} - \frac{\partial q_1}{\partial y^2} \right). \quad (37)$$

The resulting equations corresponding to equations (15) are obtained by combining equations (36) and (37). For a two-component potential, the equations corresponding to equations (16') are obtained by dropping ψ_1 terms and for a two-dimensional case by dropping ψ_1 and ψ_2 terms. Equations in orthogonal co-ordinates are obtained by dropping all g_{ij} terms where $i \neq j$.

REFERENCES

1. C. H. Wu, 'General theory of three-dimensional flows in subsonic and supersonic turbomachines', *NACA TN 2604*, 1952.
2. H. K. Cheng, 'The transonic-flow theories of high- and low-aspect-ratio wings', in T. Cebeci (ed.), *Numerical and Physical Aspects of Aerodynamic Flows*, Springer, 1982.
3. M. Hafez, 'Perturbation of transonic flows with shocks', in T. Cebeci (ed.), *Numerical and Physical Aspects of Aerodynamic Flows*, Springer, 1982.
4. M. Hafez and D. Lovell, 'Numerical solution of transonic stream function equation', *AIAA J.*, **21**, 372-336 (1983).
5. M. Hafez, J. South and E. Murman, 'Artificial compressibility methods for numerical solution of transonic full potential equation', *AIAA J.*, **17**, 838-844 (1979).

6. M. Hafez and D. Lovell, 'Improved relaxation schemes for transonic potential calculations', *AIAA Paper 83-0372*, 1983.
7. J. South, J. Keller and M. Hafez, 'Vector processor algorithms for transonic flow calculations', *AIAA J.*, **18**, 786-792 (1980).
8. N. Kemmer, *Vector Analysis*, Cambridge University Press, 1977.
9. F. Morre, 'Three dimensional compressible laminar boundary layer flow', *NACA TN 2279*, 1951.
10. M. Hafez, 'Progress in finite elements for transonic flows', *AIAA Paper 83-1919*, 1983.
11. M. Hafez and D. Lovell, 'Entropy and vorticity corrections for transonic irrotational flows', *AIAA Paper 83-1926*, 1983.
12. J. South, Private communication.
13. J. O. Bridgeman, J. L. Steger and F. T. Caradonna, 'A conservative finite difference algorithm for the unsteady transonic potential equation in generalized coordinates', *AIAA Paper 82-1388*, 1982.
14. R. Davis, J. Carter and M. Hafez, 'Three dimensional viscous flow solutions with a vorticity-stream function formulation', *AIAA Paper 87-0601*, 1987.
15. P. R. Eiseman, 'Geometric methods in computational fluid dynamics', *ICASE Report No. 80-11*, April 1980.
16. A. Rizzi and H. Viviand (eds), *Numerical Methods for the Computation of Inviscid Transonic Flows with Shock Waves*, Vieweg & John, 1981.